



# CHORUS

This is the accepted manuscript made available via CHORUS. The article has been published as:

## Dominant phonon polarization conversion across dimensionally mismatched interfaces: Carbon-nanotube-graphene junction

Jingjing Shi, Jonghoon Lee, Yalin Dong, Ajit Roy, Timothy S. Fisher, and Xiulin Ruan

Phys. Rev. B **97**, 134309 — Published 30 April 2018

DOI: [10.1103/PhysRevB.97.134309](https://doi.org/10.1103/PhysRevB.97.134309)

# Dominant phonon polarization conversion across dimensionally mismatched interfaces: carbon nanotube-graphene junction

Jingjing Shi,<sup>1</sup> Jonghoon Lee,<sup>2,3</sup> Yalin Dong,<sup>1,4</sup>

Ajit Roy,<sup>2</sup> Timothy S Fisher,<sup>5</sup> and Xiulin Ruan<sup>1,\*</sup>

<sup>1</sup>*School of Mechanical Engineering and Birck Nanotechnology Center,  
Purdue University, West Lafayette, Indiana 47907, USA*

<sup>2</sup>*Materials and Manufacturing Directorate, Air Force Research Laboratory,  
Wright-Patterson Air Force Base, Ohio 45433, USA*

<sup>3</sup>*Universal Technology Corporation, 1270 N. Fairfield Rd., Dayton, Ohio 45432, USA*

<sup>4</sup>*Department of Mechanical Engineering,  
The University of Akron, Akron, Ohio 44325, USA*

<sup>5</sup>*Department of Mechanical and Aerospace Engineering & California NanoSystems Institute,  
University of California Los Angeles, Los Angeles, CA 90095, USA*

(Dated: April 10, 2018)

## Abstract

Dimensionally mismatched interfaces are emerging for thermal management applications, but thermal transport physics remains poorly understood. Here we consider carbon nanotube-graphene junction, which is a dimensionally mismatched interface between 1D and 2D materials and is the building block for CNT-graphene 3D networks. We have predicted the transmission function of individual phonon modes using the wave packet method, surprisingly, most incident phonon modes show predominantly polarization conversion behavior. For instance, longitudinal acoustic (LA) polarizations incident from CNTs transmit mainly into flexural transverse (ZA) polarizations in graphene. The frequency stays the same as the incident mode, indicating elastic transmission. Polarization conversion is more significant as the phonon wavelength increases. We attribute such unique phonon polarization conversion behavior to the dimensional mismatch across interface, and it opens significantly new phonon transport channels as compared to existing theories where polarization conversion is neglected.

Thermal interfacial resistance is a critical issue for thermal management of modern electronic devices. Planar interfaces have been extensively studied, and theories such as the acoustic mismatch model (AMM)<sup>1</sup> have been successfully developed to predict mode-resolved phonon transport. On the other hand, dimensionally mismatched non-planar interfaces, such as 1D-2D<sup>2-6</sup>, 1D-3D<sup>7-11</sup>, and 2D-3D<sup>12-14</sup> interfaces, are emerging for many applications, but existing theories may not describe their thermal interfacial transport correctly due to new physics introduced by the dimensional mismatch. Attempt of modified acoustic mismatch model has been made at 1D-3D interface<sup>11</sup>, but has not been compared with simulation or experimental results. As an example of dimensionally mismatched interface, the current work will consider CNT-graphene junction, which is an interface between 1D and 2D materials and is the building block for CNT-graphene 3D networks recently proposed and synthesized<sup>2-6</sup>. Although CNTs<sup>13,15,16</sup> and graphene<sup>17-21</sup> have very high thermal conductivity, they both suffer from anisotropy in thermal transport. The thermal conductivity of graphene stacks or graphite in the cross-plane direction is two or more orders of magnitude lower than that of the in-plane direction<sup>22</sup>. CNT bundles also show similar behavior in the radial direction<sup>23</sup>. Therefore, the above mentioned 3D CNT-graphene network was proposed to achieve high thermal conductivity in all directions. Our previous nonequilibrium molecular dynamics (NEMD) simulations indicate that the thermal resistance in the network primarily comes from CNT-graphene junctions<sup>6</sup>. However, the NEMD method gives only an overall thermal boundary resistance without any physical insights associated with the unique dimensional mismatch nature. The CNT-graphene junctions have been synthesized in experiment<sup>5</sup>, but the interfacial thermal transport has not been measured yet. Hence, it is a timely task to understand interfacial thermal transport physics across the 1D-2D junction and assess the validity of the existing theoretical models. The results will lend useful insights for 1D-3D and 2D-3D interfaces as well.

In this work, we report the modal phonon transmission process at CNT-graphene junctions using the wave packet method<sup>4,9,24,25</sup>, which is an accurate spectral phonon transmission simulation method. The junction is between a (6, 6) CNT and graphene sheet with  $sp^2$  covalent bonds. The schematic of the simulated structure is shown in Fig. 1(a). We have found intriguing phonon polarization conversion behavior during the transmission process for all incident modes from CNT, i.e., they partially convert to different phonon polarizations in graphene after the transmission. Such surprising behavior cannot be captured by

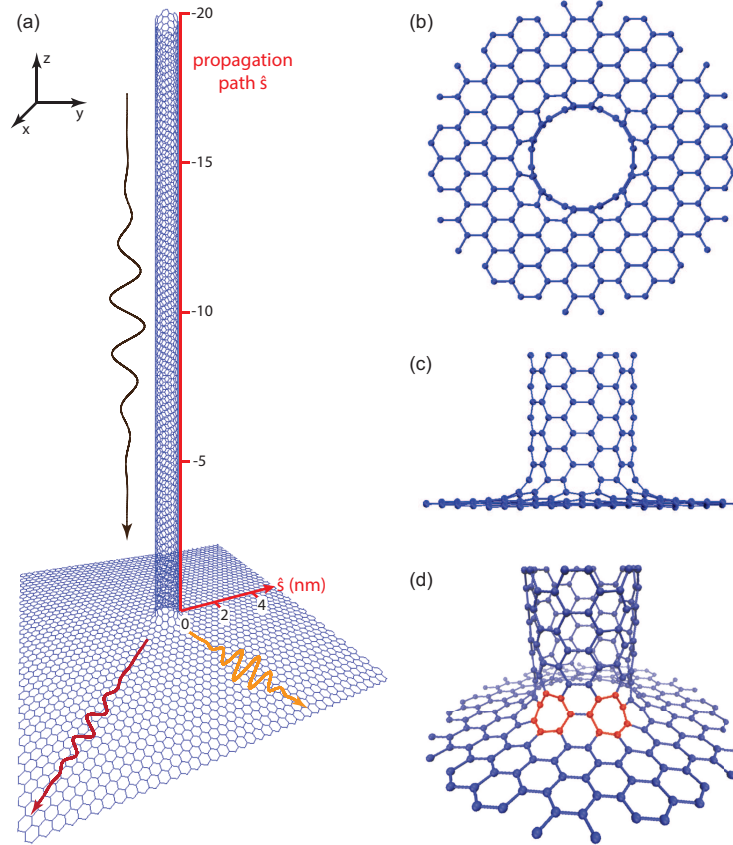


FIG. 1. (a) Schematic of the pillared graphene structure used in this work. Top view (b) and front view (c) of the detailed junction structure. (d) Detailed junction structure with perspective, where the heptagon defects are highlighted with red.

the conventional mismatch models.

## I. METHODS

The molecular dynamics (MD) phonon wave packet method is implemented with the LAMMPS package. We used the classical molecular dynamics, since only a single mode wave packet is launched in each simulation and quantum factors are not important. The detailed structure of the CNT-graphene junction is shown in Fig. 1 (b) to (d). The interactions between carbon atoms in lattice dynamics calculations and MD simulations are based on the polymer consistent force field (PCFF)<sup>26,27</sup>. The phonon dispersion relation and mode eigenvectors of (6,6) CNT are first calculated. To create a wave packet for a specific phonon mode, the initial displacement from equilibrium and velocity of the  $i$ th base atom in the  $n$ th

unit cell along the  $\alpha$  direction are<sup>4</sup>,

$$u_{ni\alpha}^\gamma = \frac{A}{\sqrt{M}} \sum_q \exp \left[ -\frac{(q - q_0)^2}{2\sigma^2} \right] \varepsilon_{i\alpha}^\gamma(q) \exp [iq(z_n - z_0)], \quad (1)$$

$$v_{ni\alpha}^\gamma = \frac{A}{\sqrt{M}} \sum_q -i2\pi v^\gamma(q) \exp \left[ -\frac{(q - q_0)^2}{2\sigma^2} \right] \varepsilon_{i\alpha}^\gamma(q) \exp [iq(z_n - z_0)], \quad (2)$$

where  $A$  is the amplitude,  $M$  is the carbon atom mass,  $q_0$  is the wavenumber of the packet,  $z_0$  and  $z_n$  are the positions of the packet center and the  $n$ th unit cell in the CNT along the propagation path  $\hat{s}$ , and  $\varepsilon$  is the eigenvector of the phonon with wavenumber  $q$  and polarization  $\gamma$ . As shown in Fig. 1(a), the phonon wave packet is activated from the CNT with a specific polarization  $\gamma$  and propagates towards the graphene sheet.

After the wave packet reaches the junction, the transmitted part continues to propagate into graphene, and the reflected part propagates back to the CNT as shown in Fig. 2(a)-(c). Monitoring the amount of energy transmitted or reflected at the junction enables the calculation of the energy transmission coefficient of the specific phonon mode. For the reflected part, the wavenumber can be calculated using the Fourier transform of atom velocity at different positions, and the frequency can be calculated using the Fourier transform of atom velocity at different time. For the transmitted part in graphene, the energy propagates in the radial direction, so the velocity of an array of atoms along the radius scaled by the square root of radius  $v \cdot \sqrt{r}$  is used in the Fourier transform. According to Parseval's theorem, the energy of each transmitted wave packet with a specific wavenumber can be calculated by the integral over the square of the amplitude of Fourier transform result. Because of the anisotropy in graphene, the transmission coefficients are different along different radial directions. Hence, both the zigzag and armchair directions are used in the Fourier transform and are averaged to determine the overall transmission coefficient. The details of the calculation of transmission coefficient can be found in supplemental material<sup>28</sup>. We have confirmed energy conservation by checking that the sum of the transmitted and reflected energies equals the incident energy.

## II. RESULTS AND DISCUSSION

In the molecular dynamics simulation, we launched wave packets of longitudinal acoustic (LA), transverse acoustic (TA), twisting (TW), and radial breathing (RB) polarizations with different wavenumbers in the CNT, because these acoustic polarizations and high group velocity polarizations are more important in thermal transport. These phonon modes are launched one at a time to predict mode-resolved transmission behavior. We find that the reflected phonon frequency, wavenumber and polarization remain the same as the incident mode, indicating an elastic reflection process. This can also be seen from Fig. 2(b), that the superposition of incident and reflected waves in the CNT near the interface has exactly the same wavelength as the incident wave packet.

However, the transmission shows surprising polarization conversion behavior, as shown in Fig. 2. The incident LA phonon polarization from CNT transmits into both LA and ZA polarizations in graphene, and the amplitude of the ZA polarization is much larger than that of the LA polarization, as shown clearly in Fig. 2(b) and (c). A video of phonon propagation can be found in supplemental material as video A<sup>28</sup>. After the Fourier transform of modified atom velocities  $v \cdot \sqrt{r}$  at different positions in graphene, two transmitted modes with their respective wavenumbers are clearly seen as two peaks in graphene  $k$ -space as shown in Fig. 3(b). Since the phonon dispersion relation of graphene has been obtained, the polarizations can be confirmed according to their frequencies and wavenumbers. Using polarization and wavenumbers, we can identify these modes as two dots on LA and ZA branches of the graphene phonon dispersion relation respectively, as shown in Fig. 3(d). Despite polarization conversion, the frequency of these transmitted modes is the same as the incident LA mode in the CNT, as shown in Fig. 3(b) and (d), indicating that the transmission process is also elastic without anharmonic phonon scattering. Hence, the transmitted LA and ZA wave packets in graphene have different wavenumbers, wavelengths, and group velocities. Fig. 2(c) clearly shows that the LA and ZA wave packets propagate at different speeds. Fig. 2(d) and (e) show the in-plane and out-of-plane atomic displacements in graphene respectively, for an incident LA wave packet. Because the graphene LA polarization only has in-plane displacement and velocity, while the ZA polarization only has out-of-plane displacement and velocity, the decomposition in Fig. 2(d) and (e) indicates that both LA and ZA modes are indeed induced in graphene. Inelastic mode conversion behaviors have been observed at silicon germanium

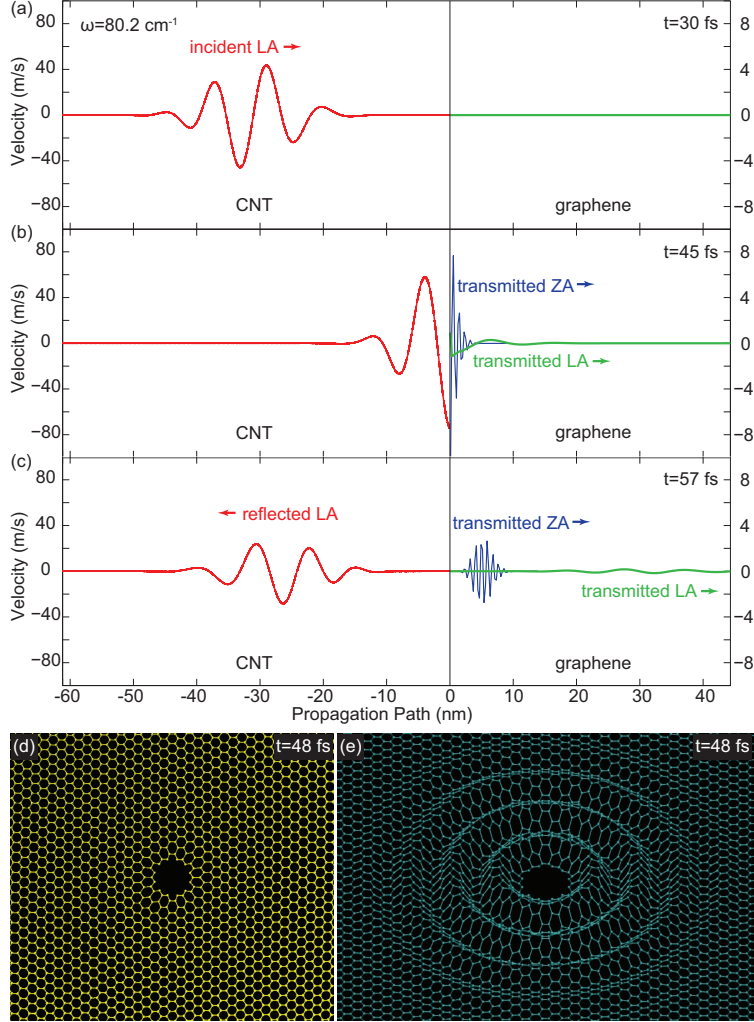


FIG. 2. Typical wave packet propagation process for an incident LA mode from CNT. Atom velocity (the left axis is the scale of atom velocity in CNT, the right axis is the scale of atom velocity in graphene) plot before the wave packet reaches the interface (a), when the wave packet just reaches the interface (b), after transmission (c). (d) In-plane displacements (amplified by 600 times) of graphenen atoms. (e) Out-of-plane displacements (amplified by 600 times) of graphene atoms.

interface with roughness<sup>25</sup> due to the anharmonic phonon scattering at the rough interface, and the effect is very small. Elastic phonon polarization conversions<sup>29,30</sup> have been observed in 3D superlattice or pure crystal for oblique incident phonon at high frequency. However, our polarization conversion at a single interface between low-dimensional materials due to dimensional mismatch is very different from these conversions. The polarization conversion we observed at CNT-graphene junction is elastic and dominates the transmission from low

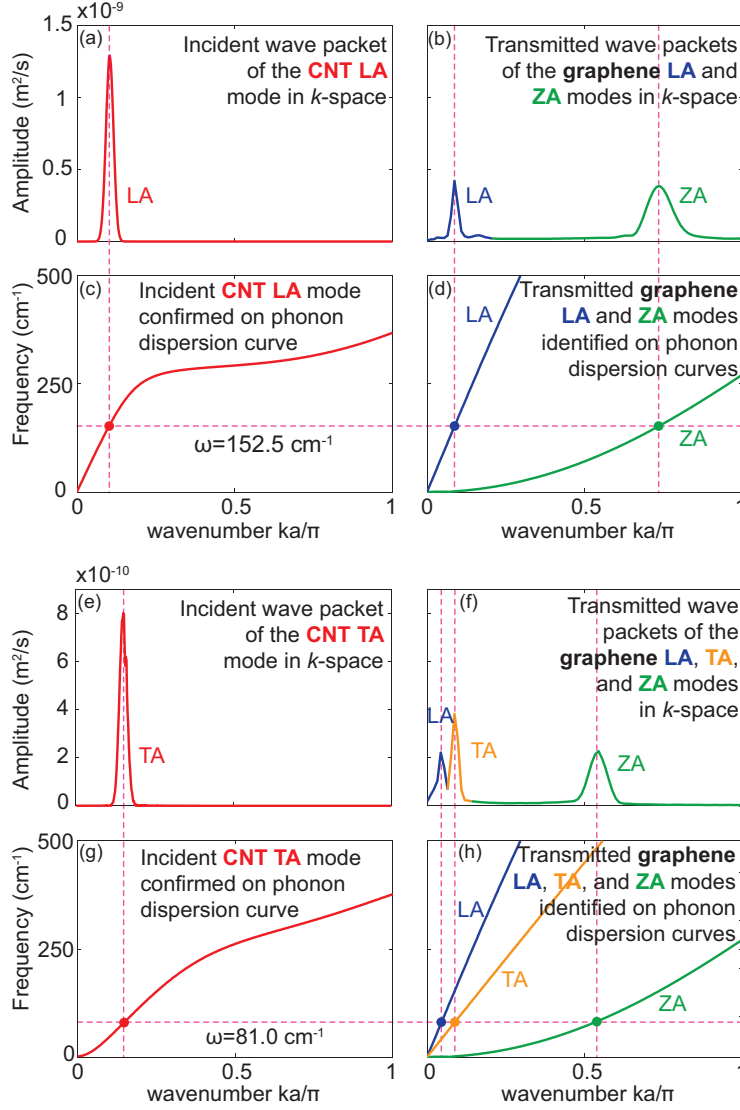


FIG. 3. An incident CNT LA wave packet (a) and its transmitted graphene LA and ZA wave packets (b) in  $k$ -space, and the corresponding identified modes on CNT LA branch (c) and graphene LA and ZA branches (d), respectively. An incident CNT TA wave packet (e) and its transmitted graphene LA, TA, and ZA wave packets (f) in  $k$ -space, and the corresponding identified modes on CNT TA branch (g) and graphene LA, TA, and ZA branches (h), respectively.

frequency to high frequency.

Like the incident LA polarization from CNT, the incident TA and other polarizations also exhibit polarization conversion behavior after transmission. For the incident TA wave packet shown in Fig. 3(e), the transmission process is more complicated since the phonon eigenvector of the CNT TA polarization not only has axial and radial components like the



LA, but also tangential component. The transmitted phonons into graphene are LA, TA, and ZA polarizations, as shown as three peaks in as shown in Fig. 3(f). The transmission process is similar to the incident LA polarization, that the frequency does not change, and transmitted modes can be identified as three dots on the LA, TA, and ZA branches of the graphene dispersion relation, as shown in Fig. 3(g) and (h). For the incident TW polarization from the CNT, the transmitted polarizations are TA and ZA because the motion of the TW polarization in the CNT is along the tangential direction, which has similar displacement as the TA polarization in graphene (in-plane transverse). For the incident RB polarization, the transmitted polarizations are LA and ZA just like the incident CNT LA polarization because the axial and radial displacements of the CNT RB polarization are similar to the displacement of the CNT LA polarization. A video of atomic vibrations of different polarizations (LA, TA, TW, and RB) in the CNT can be found in supplemental material as video B<sup>28</sup>.

We attribute the unique polarization conversion behavior across the CNT-graphene to the special dimensionally mismatched structure and defects of the system. During the transmission from one dimensional CNT to two dimensional graphene, the propagation direction of phonons must change 90 degrees as shown in Fig. 1(c), and there are six heptagonal defects as shown in Fig. 1(d). For a given incident mode such as an LA mode in CNT, some of the transmitted energy preserves the polarization without conversion, i.e. LA to LA, while the remaining transmitted energy preserves the direction of atomic vibrations or involve in some more complex process and will change polarization, i.e. LA to ZA. We suspect that the polarization conversion behavior is related to the wavelength of the incident phonon wave; hence we investigate the transmission coefficient as a function of the phonon frequency, which is directly related to the wavelength.

In Fig. 4, we show the transmission coefficient of each individual incident phonon polarization, as well as the breakdown into different transmitted polarizations in graphene. The transmission coefficient  $\Gamma_{X,\text{total}}$  is defined as the transmitted energy into the graphene over the incident energy from CNT in the polarization X. The notation  $\Gamma_{X \rightarrow Y}$  means the breakdown transmission coefficient into a specific graphene polarization Y from incident CNT polarization X. It is found that the polarization conversion is more significant for long incident wavelengths (small wavenumber). Fig. 4(a) shows that for long wavelength incident LA polarization, the transmission into the ZA polarization dominates over that into the

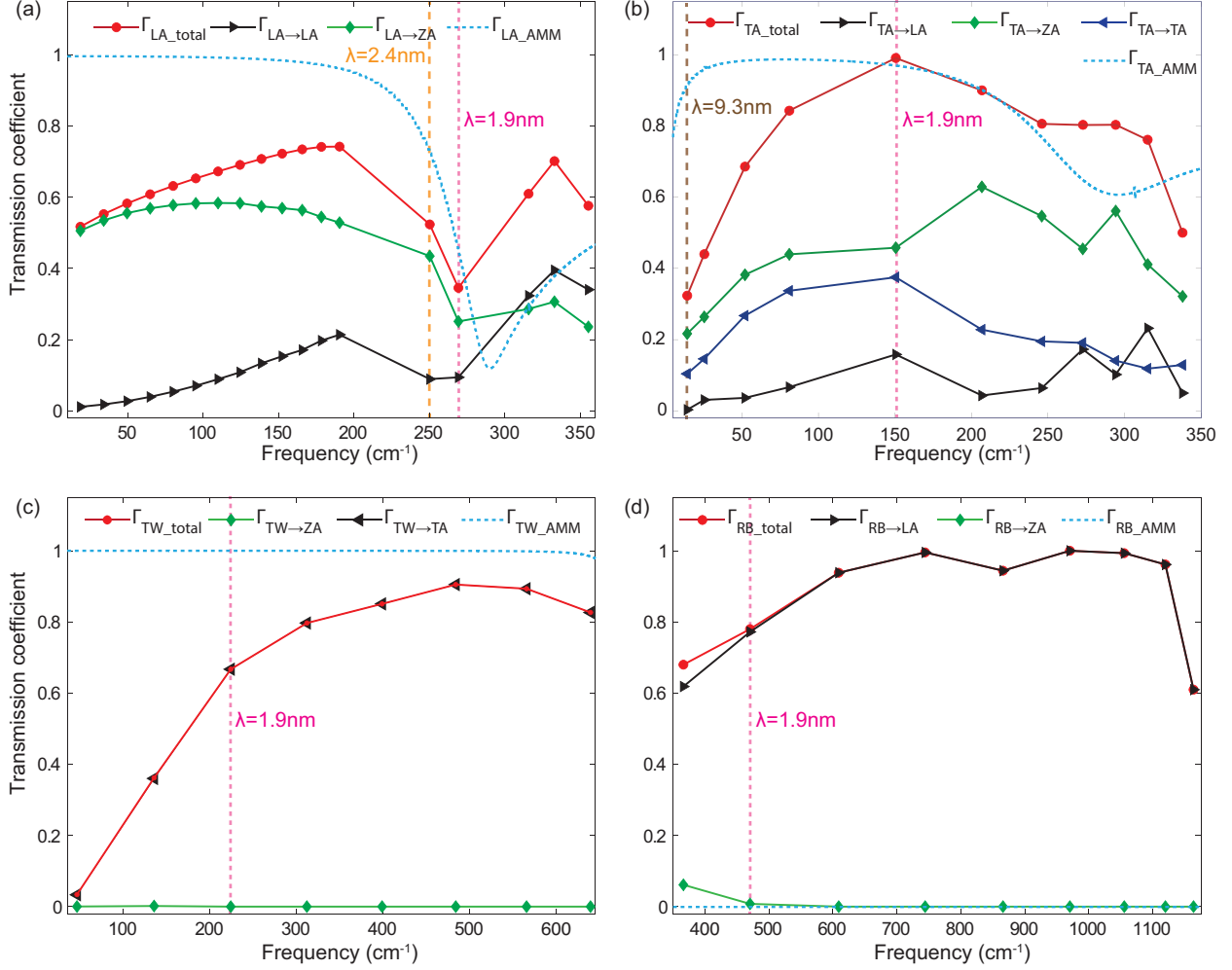


FIG. 4. Transmission coefficients of incident LA (a), TA (b), TW (c), and RB (d) polarizations.

LA polarization. It can be explained in this way. Long wavelength means the neighboring atoms in CNT vibrate almost in phase. When the motion propagates through the junction, the direction of atomic displacement (mainly along the axial direction in CNT) is largely preserved since the wavelength is much larger than the radius of curvature of the junction (about 0.5 nm). Therefore, most of the transmitted vibration becomes the ZA polarization. As the wavelength decreases, the neighboring atoms start to vibrate out of phase, and the wavelength becomes closer to the junction radius of curvature. Hence, the atomic motion originally along the axial direction in CNT can better adapt to the junction and induce more in plane ( $xy$  plane) motion in graphene. A video to describe the phenomenon is provided in supplemental material as video C<sup>28</sup>. Therefore,  $\Gamma_{LA \rightarrow LA}$  increases with decreasing wavelength.

For the incident TA polarization as shown in Fig. 4(b), the transmission into the ZA polarization dominates over that into other polarizations (LA and TA). In the long wavelength range, the polarization conversion is also more important like the incident LA polarization. About 67% of the total transmitted energy is into the ZA polarization when the frequency is about  $14 \text{ cm}^{-1}$  (wavelength  $\lambda$  is around 9.3 nm), and about 46% of the total transmitted energy is into the ZA polarization when the frequency is about  $151 \text{ cm}^{-1}$  (wavelength  $\lambda$  is around 1.9 nm). Although polarization conversion behavior dominates the transmission, the transmission process of the incident TA polarization is very different from the LA polarization. The direction of atomic displacement of the incident TA is mainly along the radial and tangential directions in CNT, while that of the transmitted ZA is along the axial direction in CNT. Hence the polarization conversion behavior like TA to ZA is a complex phenomenon that cannot be described by one simple or intuitive rule that the dominant transmitted mode will preserve the atomic vibration direction. The polarization conversion from TA to ZA might relate to the complexity of CNT TA polarization and the similarity shared by phonon dispersion relations of these two branches. For the incident TW polarization (in-plane transverse), polarization conversion to ZA (out-of-plane transverse) is more significant at long wavelength as shown in Fig. 4(c). For the incident RB polarization (atoms mainly vibrate perpendicularly to energy propagation direction), polarization conversion to LA (atoms mainly vibrate along energy propagation direction) dominates the transmission as shown in Fig. 4(d). For the incident TW and RB polarizations, most transmission preserves the atomic vibration direction.

Next we compare our simulation results to those from analytical models. Acoustic mismatch and diffuse mismatch models are commonly used for interfacial thermal transport. Here the acoustic mismatch model (AMM) is used since the  $sp^2$  covalent bond is very strong and the interface is smooth. The transmission coefficient from AMM,  $\Gamma_{X\_AMM}$ , is generally higher than the total transmission coefficient  $\Gamma_{X\_total}$  from our wave packet method especially at long wavelengths, as shown in Fig. 4. The lower transmission from the wave packet simulation can be attributed to the non-planar interface and defects (six heptagons at the interface as shown in Fig. 1). The difference between  $\Gamma_{X\_AMM}$  and  $\Gamma_{X\_total}$  at longer incident wavelength is more significant, because the junction appears to be more abrupt for longer wavelength wave packets, while it is smoother for shorter wavelength packet when the wavelength is comparable or smaller than the junction radius of curvature.

TABLE I. The CNT-graphene interface thermal conductance results predicted from Landauer approach with transmission functions from wave packet (WP) method (without and with polarization conversion) and AMM of incident LA, TA, TW, and RB branches.

Polarization	$G_{\text{WPw/o}}$ (W/m <sup>2</sup> K)	$G_{\text{WPw/}}$ (W/m <sup>2</sup> K)	$G_{\text{AMM}}$ (W/m <sup>2</sup> K)
LA	$5.02 \times 10^7$	$2.14 \times 10^8$	$2.22 \times 10^8$
TA	$1.36 \times 10^8$	$4.35 \times 10^8$	$6.18 \times 10^8$
TW	$4.64 \times 10^8$	$4.65 \times 10^8$	$1.17 \times 10^{10}$
RB	0	$9.92 \times 10^8$	0

On the other hand, from Fig. 4 (a) and (b),  $\Gamma_{\text{X}_{\text{total}}}$  is sometimes higher than  $\Gamma_{\text{X}_{\text{AMM}}}$  at certain short wavelengths (incident wavelength  $\lambda < 1.9$  nm as shown by pink dashed line). In fact, these higher  $\Gamma_{\text{X}_{\text{total}}}$  are due to polarization conversion. AMM assumes that one polarization transmits into the same polarization. However, at the CNT-graphene junction, the existence of polarization conversion provides an additional channel to transfer heat, such that  $\Gamma_{\text{X}_{\text{total}}}$  can be larger than  $\Gamma_{\text{X}_{\text{AMM}}}$ . If we compare  $\Gamma_{\text{LA}_{\text{AMM}}}$  to  $\Gamma_{\text{LA} \rightarrow \text{LA}}$  alone for the incident LA polarization, we can see that  $\Gamma_{\text{LA}_{\text{AMM}}}$  is indeed generally higher than  $\Gamma_{\text{LA} \rightarrow \text{LA}}$  especially at long wavelength. The difference between  $\Gamma_{\text{LA}_{\text{AMM}}}$  and  $\Gamma_{\text{LA}_{\text{total}}}$  when  $\lambda < 1.9$  nm is completely from polarization conversion  $\Gamma_{\text{LA} \rightarrow \text{ZA}}$ . Interestingly, when compared with the transmission coefficient from one polarization to the same one, AMM can still capture some features of transmission. For example,  $\Gamma_{\text{LA} \rightarrow \text{LA}}$  shows a minimum at around  $250 \text{ cm}^{-1}$  (wavelength  $\lambda=2.4$  nm), and  $\Gamma_{\text{LA}_{\text{AMM}}}$  also shows a minimum at around  $290 \text{ cm}^{-1}$ . This minimum from AMM is due to the large mismatch in the group velocities of CNT and graphene, which can be found from the phonon dispersion relation FIG. S2 in supplemental material<sup>28</sup>.

To understand how the polarization conversion affects thermal conductance, we have applied the Landauer formula<sup>31</sup> with the above transmission functions from wave packet and AMM respectively to calculate thermal conductance at the pillared graphene interface, and compare the results. The Landauer formula is

$$q = \frac{1}{2\pi} \int_0^{+\infty} \hbar\omega [M_1(\omega)\tau_{1 \rightarrow 2}(\omega)f(T_1) - M_2(\omega)\tau_{2 \rightarrow 1}(\omega)f(T_2)]d\omega, \quad (3)$$

where  $M(\omega)$  is the number of modes at a given frequency  $\omega$ ,  $\tau(\omega)$  is the transmission coefficient at the interface from one material to the other, and  $f(T)$  is the Bose-Einstein

distribution function at temperature  $T$ . The equivalent equilibrium temperature correction<sup>32</sup> is used since the transmission coefficients are high at CNT-graphene junction. As shown clearly in Table. I, for the incident LA polarization, the polarization conversion increases the conductance from  $5.02 \times 10^7$  W/m<sup>2</sup>K to  $2.14 \times 10^8$  W/m<sup>2</sup>K. The contribution of polarization conversion is 76.5% of the total conductance. For the incident TA polarization as shown in Table. I, the contribution of polarization conversion, which is 68.7% of the total also dominates. Interestingly, for the incident RB polarization, since there is no corresponding polarization in graphene, the conductance without polarization conversion is 0, and the contribution of polarization conversion is 100%. When compared with conductance results from AMM transmission coefficients,  $G_{LA\_WP}$  is comparable to  $G_{LA\_AMM}$  because  $\Gamma_{LA\_total}$  is generally smaller than  $\Gamma_{LA\_AMM}$ , but larger than  $\Gamma_{LA\_AMM}$  at high frequency. For TA and TW branches,  $G_{WP}$  is smaller than  $G_{AMM}$  since the transmission  $\Gamma_{total}$  is generally smaller than  $\Gamma_{AMM}$ . For RB branch, as we mentioned above, since there is no corresponding polarization in graphene,  $G_{RB\_AMM}$  is 0, and  $G_{RB\_WP}$  is much larger than it. From the interface thermal conductance calculation, it shows that polarization conversion dominates most incident phonon polarizations, and the interface conductance with transmission from wave packet  $G_{WP}$  can be smaller than  $G_{AMM}$  when the transmission is smaller, and can also exceed  $G_{AMM}$  because the former includes while the latter neglects polarization conversion. Therefore, the unique junction between 1D CNT and 2D graphene on one hand tends to reduce the transmission and interface conductance due to the defects and dimensional mismatch, while on the other hand tends to enhance the transmission and conductance due to polarization conversion. The overall effect depends on which mechanism dominates.

### III. SUMMARY AND CONCLUSIONS

To summarize, we have predicted the transmission function of individual phonon mode using the wave packet method at CNT-graphene junction, which is a dimensionally mismatched interface between 1D and 2D materials. Intriguing phonon polarization conversion behavior is observed for most incident phonon modes. Polarization conversion is found to dominate the transmission and is more significant at larger phonon wavelength. We attribute such unique phonon polarization conversion behavior to the dimensional mismatch and defects across CNT-graphene interface. The polarization conversion is a complicated

phenomenon related to interface atomic structure, phonon polarization, direction of atomic displacement, phonon dispersion relations. As such, the transmission functions and interfacial conductance at the junction cannot be explained by the conventional acoustic mismatch models. The dimensionally mismatched interface on one hand tends to reduce the transmission and conductance due to defects and the change of phonon propagation direction, while on the other hand tends to enhance the transmission and conductance due to the new phonon transport channel introduced by polarization conversion.

## ACKNOWLEDGMENTS

The authors would like to acknowledge the support by the Air Force Office of Scientific Research (AFOSR) MURI grant (FA9550-12-1-0037).

---

\* ruan@purdue.edu

- <sup>1</sup> E. T. Swartz and R. O. Pohl, *Reviews of Modern Physics* **61**, 605 (1989).
- <sup>2</sup> G. K. Dimitrakakis, E. Tylianakis, and G. E. Froudakis, *Nano Letters* **8**, 3166 (2008).
- <sup>3</sup> V. Varshney, A. K. Roy, G. Froudakis, and B. L. Farmer, *Nanoscale* **3**, 3679 (2011).
- <sup>4</sup> J. Lee, V. Varshney, J. S. Brown, A. K. Roy, and B. L. Farmer, *Applied Physics Letters* **100**, 183111 (2012).
- <sup>5</sup> Y. Xue, Y. Ding, J. Niu, Z. Xia, A. Roy, H. Chen, J. Qu, Z. L. Wang, and L. Dai, *Science Advances* **1**, e1400198 (2015).
- <sup>6</sup> J. Shi, Y. Dong, T. Fisher, and X. Ruan, *Journal of Applied Physics* **118**, 044302 (2015).
- <sup>7</sup> I. Duchemin and D. Donadio, *Physical Review B - Condensed Matter and Materials Physics* **84**, 1 (2011), arXiv:1103.5581.
- <sup>8</sup> B. A. Cola, J. Xu, C. Cheng, X. Xu, T. S. Fisher, and H. Hu, *Journal of Applied Physics* **101** (2007), 10.1063/1.2510998.
- <sup>9</sup> M. Hu, P. Keblinski, J. S. Wang, and N. Raravikar, *Journal of Applied Physics* **104** (2008), 10.1063/1.3000441.
- <sup>10</sup> Y. Wang, X. Ruan, and A. K. Roy, *Physical Review B* **85**, 205311 (2012).
- <sup>11</sup> R. Prasher, T. Tong, and A. Majumdar, *Journal of Applied Physics* **102**, 104312 (2007).

- <sup>12</sup> J. H. Seol, I. Jo, A. L. Moore, L. Lindsay, Z. H. Aitken, M. T. Pettes, X. Li, Z. Yao, R. Huang, D. Broido, N. Mingo, R. S. Ruoff, and L. Shi, *Science* (New York, N.Y.) **328**, 213 (2010).
- <sup>13</sup> B. Qiu, Y. Wang, Q. Zhao, and X. Ruan, *Applied Physics Letters* **100** (2012), 10.1063/1.4725194.
- <sup>14</sup> Z. Wang, T. Feng, and X. Ruan, *Journal of Applied Physics* **117** (2015), 10.1063/1.4913600.
- <sup>15</sup> J. Shiomi and S. Maruyama, *Physical Review B* **73**, 205420 (2006).
- <sup>16</sup> L. Lindsay, D. A. Broido, and N. Mingo, *Physical Review B* **82**, 161402 (2010).
- <sup>17</sup> A. A. Balandin, S. Ghosh, W. Bao, I. Calizo, D. Teweldebrhan, F. Miao, and C. N. Lau, *Nano Letters* **8**, 902 (2008).
- <sup>18</sup> S. Ghosh, I. Calizo, D. Teweldebrhan, E. P. Pokatilov, D. L. Nika, A. A. Balandin, W. Bao, F. Miao, and C. N. Lau, *Applied Physics Letters* **92**, 151911 (2008).
- <sup>19</sup> L. Lindsay, D. A. Broido, and N. Mingo, *Physical Review B* **82**, 115427 (2010).
- <sup>20</sup> J. Hu, X. Ruan, and Y. P. Chen, *Nano Letters* **9**, 2730 (2009).
- <sup>21</sup> Y. Wang, B. Qiu, and X. Ruan, *Applied Physics Letters* **101**, 13101 (2012).
- <sup>22</sup> A. A. Balandin, *Nature Materials* **10**, 569 (2011).
- <sup>23</sup> J. Che, T. Cagin, and W. Goddard, *Nanotechnology* **11**, 65 (2000).
- <sup>24</sup> Z. T. Tian, B. E. White, and Y. Sun, *Applied Physics Letters* **96**, 263113 (2010).
- <sup>25</sup> L. Sun and J. Y. Murthy, *Journal of Heat Transfer* **132**, 102403 (2010).
- <sup>26</sup> H. Sun, S. J. Mumby, J. R. Maple, and A. T. Hagler, *Journal of the American Chemical Society* **116**, 2978 (1994).
- <sup>27</sup> H. Sun, *Journal of Physical Chemistry B* **5647**, 7338 (1998).
- <sup>28</sup> See Supplemental Material at [URL will be inserted by publisher] for more details of the phonon wave packet propagation process and the calculation of transmission coefficients.
- <sup>29</sup> Hatsuyoshi Kato, H. Maris, and S. Tamura, *Physica B: Condensed Matter* **219-220**, 696 (1996).
- <sup>30</sup> A. G. Every, W. Sachse, K. Y. Kim, and M. O. Thompson, *Physical Review Letters* **65**, 1446 (1990).
- <sup>31</sup> T. S. Fisher, in *Thermal Energy at the Nanoscale* (WORLD SCIENTIFIC, 2013) pp. 87–111.
- <sup>32</sup> T. Zeng, Gang Chen, *Microscale Thermophysical Engineering* **5**, 71 (2001).